

# Constitutive Expression of Short Hairpin RNA *in Vivo* Triggers Buildup of Mature Hairpin Molecules

M. Ahn,<sup>1,\*</sup> S.R. Witting,<sup>1,\*</sup> R. Ruiz,<sup>1</sup> R. Saxena,<sup>2</sup> and N. Morral<sup>1,3</sup>

## Abstract

RNA interference (RNAi) has become the cornerstone technology for studying gene function in mammalian cells. In addition, it is a promising therapeutic treatment for multiple human diseases. Virus-mediated constitutive expression of short hairpin RNA (shRNA) has the potential to provide a permanent source of silencing molecules to tissues, and it is being devised as a strategy for the treatment of liver conditions such as hepatitis B and hepatitis C virus infection. Unintended interaction between silencing molecules and cellular components, leading to toxic effects, has been described *in vitro*. Despite the enormous interest in using the RNAi technology for *in vivo* applications, little is known about the safety of constitutively expressing shRNA for multiple weeks. Here we report the effects of *in vivo* shRNA expression, using helper-dependent adenoviral vectors. We show that gene-specific knockdown is maintained for at least 6 weeks after injection of  $1 \times 10^{11}$  viral particles. Nonetheless, accumulation of mature shRNA molecules was observed up to weeks 3 and 4, and then declined gradually, suggesting the buildup of mature shRNA molecules induced cell death with concomitant loss of viral DNA and shRNA expression. No evidence of well-characterized innate immunity activation (such as interferon production) or saturation of the exportin-5 pathway was observed. Overall, our data suggest constitutive expression of shRNA results in accumulation of mature shRNA molecules, inducing cellular toxicity at late time points, despite the presence of gene silencing.

## Introduction

**R**NA INTERFERENCE (RNAi) is a cellular mechanism to inhibit expression of gene products in a highly specific manner. Double-stranded RNA (dsRNA) is recognized by Dicer, a ribonuclease III (RNase III) enzyme, which cleaves the dsRNA into 21- to 23-nucleotide small interfering RNAs (siRNAs). On loading onto the RNA-induced silencing complex (RISC), one of the two strands is selected (referred to as the guide strand) and the other one is degraded (passenger strand) (Matranga *et al.*, 2005). The RISC–siRNA complex binds to mRNA targets and triggers their degradation through Argonaute (AGO)-mediated cleavage (Liu *et al.*, 2004; Song *et al.*, 2004). Compared with siRNA delivery, short hairpin RNA (shRNA) expression has the advantage of providing a continuous source of silencing molecules and is a potent experimental tool for long-term gene silencing (Brummelkamp *et al.*, 2002; McIntyre and Fanning, 2006). Constitutive synthesis of shRNA is being pursued to treat genetic conditions such as Huntington's disease (Boudreau *et al.*, 2009), or chronic viral infections

such as hepatitis B virus (Grimm and Kay, 2006; Giering *et al.*, 2008). In addition to its use as a gene therapy treatment, constitutive shRNA expression has ample applications in gene function studies, in particular *in vivo*, as it allows shortening the time-consuming process of generating tissue-specific null animals. Expression of shRNA has had an enormous impact on accelerating discovery of therapeutic targets (Colombo and Moll, 2008; Ruiz *et al.*, 2009).

The liver is a crucial tissue implicated in the control of glucose and lipid homeostasis, and the target tissue for functional studies directed at studying the molecular mechanisms leading to prevalent conditions such as type 2 diabetes, metabolic syndrome, and cardiovascular disease. Adenoviruses are highly efficient vectors for delivery of genes into the liver. The feasibility of silencing gene expression in animal models, using this vector system, has been shown in multiple studies (Xia *et al.*, 2002; Taniguchi *et al.*, 2005; Narvaiza *et al.*, 2006). Nevertheless, all these studies used first-generation (E1-deleted) adenoviral vectors, which are highly hepatotoxic at high doses and immunogenic,

<sup>1</sup>Department of Medical and Molecular Genetics, <sup>2</sup>Department of Pathology, and <sup>3</sup>Department of Biochemistry and Molecular Biology, Indiana University School of Medicine, Indianapolis, IN 46202.

\*M.A. and S.R.W. contributed equally to this work.

leading to clearance of transduced cells (Yang *et al.*, 1994; Morral *et al.*, 1997). In addition, these vectors express VA1 noncoding RNA, which inhibits microRNA processing by interfering with nuclear export and Dicer functionality (Lu and Cullen, 2004). The use of helper-dependent adenoviral vectors (also known as “gutless” or high-capacity vectors), devoid of viral genes, has been shown to overcome these problems (Schiedner *et al.*, 1998; Morral *et al.*, 1999; O’Neal *et al.*, 2000). Helper-dependent adenoviruses conserve the advantages of early-generation adenovirus vectors, including high-efficiency *in vivo* transduction and high-level transgene expression, with the added features of long-term gene expression and negligible cytotoxicity at high doses. We have previously shown 75–90% gene silencing in short-term *in vivo* experiments (Witting *et al.*, 2008; Ruiz *et al.*, 2009).

Despite the enormous potential of RNAi as a therapeutic treatment and as a tool in functional studies, unintended interactions between the silencing molecule and cellular components occur (known as nonspecific effects). Administration of high doses of siRNA can result in nonspecific events due to activation of innate immune responses such as the interferon response, through poorly understood molecular mechanisms (Robbins *et al.*, 2008). Induction of this response is siRNA concentration dependent (Persengiev *et al.*, 2004) and cell type dependent (Reynolds *et al.*, 2006), which indicates that data generated in one cell type may not apply to a different one, and that studies need to be conducted in the cell/tissue of interest. In addition, it has been shown that cells have a limited capacity to process shRNA, and that oversaturation of the exportin-5 pathway (necessary to transport shRNA to the cytoplasm) by high-level shRNA expression results in downregulation of endogenous microRNAs, inducing cell death (Grimm *et al.*, 2006). Our studies have shown that constitutive expression of shRNA induces interferon responses in a sequence and adenovirus dose-dependent manner (Witting *et al.*, 2008). Altogether these data clearly indicate that the successful establishment of RNA interference as a universal tool to study gene function and for clinical applications requires a better understanding of shRNA processing *in vivo*.

We have reported that it is possible to express shRNA from the U6 promoter and to induce gene silencing in liver for up to 3 weeks in the absence of interferon responses (Ruiz *et al.*, 2009). To study the feasibility of constitutively expressing shRNA for multiple weeks, we analyzed the impact on target gene expression, endogenous microRNA levels, as well as expression of interferon-responsive genes. Our data suggest that constitutive shRNA expression results in effective processing of hairpin molecules. Nevertheless, mature hairpin molecules accumulate to an extent that eventually induces cellular toxicity.

## Materials and Methods

### Helper-dependent adenoviral vector production

Cloning and rescue of helper-dependent adenoviral vectors gAd.shSREBP1, gAd.shSCR, and gAd.NEC have been described previously (Witting *et al.*, 2008; Ruiz *et al.*, 2009). All these vectors are based on serotype 5 adenovirus, which transduces hepatocytes efficiently (Stratford-Perricaudet *et al.*, 1990) and can infect hepatic stellate cells (Inagaki *et al.*, 2005) and macrophages (Wheeler *et al.*, 2001), but poorly transduces si-

nusoidal endothelial cells (Hegenbarth *et al.*, 2000). Large-scale preparations of these three vectors were obtained in 293Cre4 cells (Microbix Biosystems, Toronto, ON, Canada) (Parks *et al.*, 1996), following a previously described protocol (Ruiz *et al.*, 2009). Briefly, 293Cre4 cells grown at 95% confluency in 15 triple flasks (500 cm<sup>2</sup>; 5–7 × 10<sup>7</sup> cells per flask) were infected with helper-dependent vector at a multiplicity of infection (MOI) of 3 and with helper H14 at an MOI of 2. Cells were incubated at 37°C in a 5% CO<sub>2</sub> atmosphere, and were harvested in the presence of >90% cytopathic effect (CPE). The virus was purified by one CsCl step gradient centrifugation followed by one CsCl isopycnic separation. The helper-dependent adenovirus band was collected and dialyzed in TMN buffer (10 mM Tris-HCl [pH 7.5], 1 mM MgCl<sub>2</sub>, 150 mM NaCl, 10% glycerol). Total viral particles were determined spectrophotometrically after particle disruption with 0.1% sodium dodecyl sulfate (SDS) (absorbance at 260 nm [*A*<sub>260</sub>] = 1 corresponds to 1.1 × 10<sup>12</sup> viral particles/ml). Stocks were stored at –80°C and diluted in TMN buffer for *in vivo* administration.

### Animals

Male 8-week-old C57BL/6J mice were obtained from Jackson Laboratory (Bar Harbor, ME). Animal care guidelines set forth by the Indiana University School of Medicine (Indianapolis, IN) were followed. Mice were kept in a BL2 facility and had access to standard chow and water *ad libitum*. Mice received 1 × 10<sup>11</sup> viral particles (VP) of gAd.shFABP5, gAd.shSREBP1, gAd.shSCR, gAd.NEC, or vehicle in a volume of 250 μl, by tail vein injection. Animals were killed at the times indicated in text. Livers were collected and snap-frozen in liquid nitrogen or fixed in 10% formalin buffer for histological analysis. Serum was obtained and frozen at –20°C.

### Alanine aminotransferase test

Serum alanine aminotransferase was tested with a liquid ALT (SGPT) reagent set (Pointe Scientific, Canton, MI). Twenty microliters was used for the analysis, in accordance with the manufacturer’s instructions.

### Western blotting

Liver protein extracts were generated by tissue homogenization in radioimmunoprecipitation assay (RIPA) buffer containing protein inhibitors (50 mM Tris, 150 mM NaCl, 1 mM EDTA, 0.25% [w/v] deoxycholate, 1% Triton X-100, 1 mM phenylmethylsulfonyl fluoride [PMSF], aprotinin/leupeptin/pepstatin [1 μg/ml]; pH 7.5). Protein concentration was measured with a bicinchoninic acid (BCA) kit (Pierce, Rockford, IL). Forty micrograms of protein was loaded in 10 or 15% SDS–polyacrylamide Criterion gels (Bio-Rad, Hercules, CA) and transferred to 0.2-μm polyvinylidene difluoride (PVDF) membranes. Blocking was performed in TBS-T (20 mM Tris, 150 mM NaCl, 0.1% Tween 20; pH 7.5) with 5% blocking-grade milk (Bio-Rad). Primary antibodies against sterol regulatory element binding protein-1 (SREBP1) (Santa Cruz Biotechnology, Santa Cruz, CA), Eri-1 (Santa Cruz Biotechnology), fatty acid binding protein-5 (FABP5) (R&D Systems, Minneapolis, MN), α-tubulin (Millipore, Temecula, CA), and cyclophilin-40 (Abcam, Cambridge, MA) were diluted in blocking solution and incubated for 2 hr at room temperature (α-tubulin) or overnight at 4°C (SREBP-1,

Eri-1, FABP5, and cyclophilin 40). Secondary antibody incubations were carried out for 1 hr at room temperature. Blots were developed with an enhanced chemiluminescence (ECL) kit (Thermo Fisher Scientific, Waltham, MA) and exposed to enhanced chemiluminescence film (GE Healthcare, Piscataway, NJ).

#### RNA isolation and Northern blot analysis

RNA was isolated from approximately 100 mg of frozen liver tissue, using a *mirVana* RNA isolation kit (Ambion, Austin, TX) according to the manufacturer's instructions. mRNA and microRNA (miRNA)-enriched RNA fractions were obtained. RNA concentration was determined by light absorption at 260 nm ( $A_{260}$ ), using a NanoDrop 2000 spectrophotometer (Thermo Scientific, Waltham, MA). Six micrograms of miRNA-enriched RNA was heated for 5 min at 95°C. Samples were separated on 15% TBE-urea gels (Bio-Rad), transferred to Hybond N+ membranes (GE Healthcare) at 10 V for 1.5 hr, and UV-cross-linked with a Stratilinker 2400 (Stratagene/Fisher Scientific, La Jolla, CA). Sequences of the DNA oligonucleotide probes used are shown in Table 1. RNA oligonucleotides with the sequence of the precursor shRNA (50-nucleotide) sequence, or the mature SREBP (21-nucleotide) sequence, were used as controls to determine the size of the shRNA produced *in vivo*. For hybridization, DNA oligonucleotide probes (100 pmol) were labeled with digoxigenin-labeled deoxyuridine-triphosphate (DIG-dUTP), using a DIG oligonucleotide tailing kit, second generation (Roche Diagnostics, Mannheim, Germany). Membranes were prehybridized for 2 hr at 60°C. Probes were hybridized to membranes at 25°C overnight in a hybridization oven. After hybridization, membranes were briefly washed and incubated for 30 min in blocking solution. Blots were subjected to

immunological detection, using anti-digoxigenin antibody conjugated to alkaline phosphatase (AP) (Roche Diagnostics). The signal was developed with a CSPD ready-to-use kit (Roche Diagnostics).

#### qRT-PCR

The mRNA-enriched fraction (described previously) was treated with RNase-free DNase (Qiagen, Germantown, CA) to remove contaminant DNA. The concentration of the RNA was determined in the NanoDrop 2000, and the  $A_{260}/A_{280}$  ratio was between 1.9 and 2.1. mRNA quantification was performed by real-time RT-PCR, using a SYBR green Qiagen one-step RT-PCR kit (Qiagen, Valencia, CA) in accordance with the manufacturer's protocol. qRT-PCR was carried out with an ABI 7500 instrument (Applied Biosystems, Foster City, CA). Primer pairs were designed to bind different exons of the gene and amplify fragments of approximately 200 bp, and were first confirmed to yield a single band of the expected size by agarose gel electrophoresis, as well as a negative result in wells containing sample without reverse transcriptase (RT-). Primer pairs were synthesized by Invitrogen (Carlsbad, CA) and are described in Table 1. A standard curve was generated with serial dilutions of an RNA sample from a vehicle-treated mouse (200 ng down to 6.25 ng). Test samples were diluted to 25 ng/ $\mu$ l and quantification of mRNA levels was done by analyzing 50 ng of RNA, in duplicate, in a 50- $\mu$ l reaction volume and using a 0.5  $\mu$ M concentration of each primer. Threshold cycle ( $C_t$ ) values were compared with those of the standard curve. Aldolase A was used as loading control gene. This gene was selected on the basis of the absence of statistically significant differences between the groups. Fold changes are expressed relative to the gAd.NEC-treated group. This group was used as reference after confirming that levels of all genes analyzed were not significantly different from the vehicle-treated group (data not shown). All gAd.NEC, gAd.shSREBP1, and gAd.shSCR samples were analyzed in the same 96-well plate.

#### Microarray analysis

Samples (three per group) were labeled as per the standard Affymetrix protocol for the WT sense target labeling and control reagents kit according to the Affymetrix user manual *GeneChip Whole Transcript (WT) Sense Target Labeling Assay*. Individual labeled samples were hybridized to the GeneChip Mouse Gene 1.0 ST array for 17 hr and then washed, stained, and scanned according to the standard protocol, using the Affymetrix GeneChip operating system (GCOS). GCOS was used to generate data (CEL files). Arrays were visually scanned for abnormalities or defects. CEL files were imported into the Partek genomics suite (Partek, St. Louis, MO). RMA (robust multichip average) signals were generated for the core probe sets, using the RMA background correction, quantile normalization, and summarization by median polish. Summarized signals for each probe set were  $\log_2$  transformed. These  $\log_2$ -transformed signals were used for principal components analysis, hierarchical clustering, and signal histograms to determine whether there were any outlier arrays. Untransformed RMA signals were used for fold change calculations. Data were analyzed by one-way analysis of variance (ANOVA), using  $\log_2$ -transformed signals with treatment as factor and all

TABLE 1. OLIGONUCLEOTIDE SEQUENCES

<b>Primers for qRT-PCR (5' → 3')</b>	
ISG56:	AGAGAACAGCTACCACCTTT (F) TGGACCTGCTCTGAGATTCT (R)
OAS1b:	TTGATGTGCTGCCAGCCTAT (F) TGAGGCGCTTCAGCTTGGTT (R)
Eri-1:	ATCGAAGTTCATTTCCCTCCAATGG (F) TCATAGTAACTGTCCCCAGCGG (R)
AldoA:	GAGCAGAAGAAGGAGCTGTC (F) GTCTCGTGGAAGAGGATCAC (R)
<b>Primers for vector genome qPCR (5' → 3')</b>	
pSHL:	GCGTGCCAGACAAAAGGAAAG (F) CACTCCAGCAGCCCAGAATC (R)
GK:	GGACCAGAGGCTCCTTACCT (F) ACCAGCTTGAGCAGCACAAG (R)
<b>Oligonucleotides for Northern blot (5' → 3')</b>	
5S RNA:	TTAGCTCCGAGATCA
SCR-as:	ACTTGACCTCCTTATACTCTC
SCR-s:	GAGAGTATAAGGAGGTCAAGT
SREBP1-as:	AGTTTGTCTGTGTCCACAACC
SREBP1-s:	GGTTGTGGACACAGACAAACT
miR122-as:	TGGAGTGTGACAATGGTGTGTTGT
miR122-s:	ACAAACACCATTTGTCACACTCCA

ISG56, interferon-stimulated gene 56; OAS1b, 2',5'-oligoadenylate synthetase 1b; ISG20, interferon-stimulated gene 20; Aldo A, aldolase A; pSHL, shuttle plasmid for rescue of helper-dependent adenoviral vectors; GK, glucokinase; as, antisense; s, sense.



possible contrasts made. Fold changes were calculated using the untransformed RMA signals. Gene expression comparisons were made between shSCR (scrambled shRNA sequence) versus NEC control and shSREBP1 (shRNA knocking down SREBP1 expression) versus NEC control, and only genes changing in the same direction in both comparisons with  $p < 0.01$  and false discovery rate  $< 0.05$  were considered. A total of 2016 genes were upregulated and 577 were downregulated. To identify pathways/processes in which these genes are implicated, 1.5-fold upregulated genes (868) and 1.5-fold downregulated genes (216) were classified by functional annotation clustering (NIH DAVID [Database for Annotation, Visualization, and Integrated Discovery] database; Huang *et al.*, 2009) and a medium- or high-stringency level. Only clusters with an enrichment score  $\geq 1.3$  were considered.

#### Vector genome copy number

Genomic DNA was extracted from approximately 100 mg of frozen tissue, using a Qiagen genomic kit. Helper-dependent adenoviral vector genome copy number was quantified by real-time PCR, using an ABI 7500 instrument (Applied Biosystems) and a power SYBR green kit (Applied Biosystems) in accordance with the manufacturer's protocol. Vector DNA quantification was done as previously described (Ruiz *et al.*, 2009), using a  $0.5 \mu\text{M}$  concentration of a primer pair specific to the backbone sequence in the helper-dependent vector genome, and primers specific to the glucokinase gene, used as loading control (Table 1). A standard curve was generated by spiking DNA, isolated from a mouse treated with vehicle, with known amounts of pSHL-GFP plasmid to generate a standard curve with 0.01, 0.1, 1, 10, and 100 copies per cell. DNA levels in standards and test samples were measured by analyzing 30 ng of DNA, in duplicate. After adjusting for glucokinase levels, the genome copy number of each sample was determined by regression analysis.

#### Histology

Four-micron-thick sections were cut from paraffin-embedded tissue and stained with hematoxylin and eosin for histological analysis. Processing and staining were performed at the Immunohistochemistry Core (IHC) at Indiana University Medical Center (Indianapolis, IN). Liver sections were analyzed by an experienced liver pathologist (R.S.) in a blinded fashion.

#### Statistical analysis

Numerical data represent means  $\pm$  SD. Significant differences are defined as  $p < 0.05$  by two-tailed, unpaired  $t$  test.

### Results

#### Gene silencing is maintained over time

We have previously reported that administration of  $1 \times 10^{11}$  VP of gAd.shFABP5 (expressing an shRNA to knock down fatty acid binding protein-5 [FABP5]) resulted in 75% gene silencing 1 week after vector administration (Witting *et al.*, 2008). To study the feasibility of expressing shRNA for multiple weeks in liver, C57BL/6 mice were given  $1 \times 10^{11}$  VP of gAd.shFABP5 or gAd.shSCR (expressing a scrambled sequence), and were killed after 1 or 8 weeks. A significant

level of silencing was maintained at week 8 compared with week 1 (Fig. 1), suggesting it is possible to obtain stable knockdown with helper-dependent adenoviral vectors.

#### Constitutive shRNA expression leads to liver cell damage

To determine whether these observations were reproduced with a vector targeting a different gene and to study in more detail the effects of expressing shRNA for multiple weeks, C57BL/6 mice were injected  $1 \times 10^{11}$  VP of gAd.shSREBP1 (expressing an shRNA to knock down the transcription factor sterol regulatory element binding protein-1 [SREBP1]) or gAd.shSCR. As controls for shRNA expression, groups of mice received gAd.NEC (no expression cassette) or vehicle. Mice were killed 1, 3, and 6 weeks postinjection. SREBP-1 knockdown was observed at weeks 1 and 3 and was maintained at week 6 (Fig. 2A). Surprisingly, quantification of adenoviral vector genome copy number revealed a significant decrease between weeks 3 and 6 with both shRNA-expressing vectors (gAd.shSCR and gAd.shSREBP1) (Fig. 2B). This correlated with an increase in ALT levels, a marker of liver damage (Fig. 2C). No difference in vector genome copy number was observed in animals treated with gAd.NEC, indicating the loss of vector DNA was not due to toxicity from the helper-dependent adenoviral vector itself, but was associated with shRNA expression.

#### Loss of vector DNA correlates with shRNA accumulation in the liver

To determine whether vector DNA correlated with level of shRNA, the microRNA-enriched RNA fraction was isolated

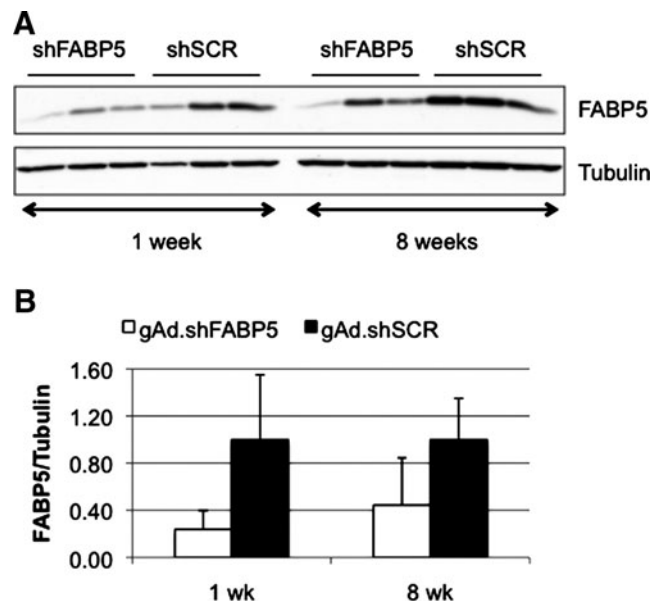


**FIG. 1.** Gene silencing is maintained over time. Mice were given  $1 \times 10^{11}$  VP of gAd.shFABP5 or gAd.shSCR intravenously ( $n = 3$ ). Animals were killed 1 or 8 weeks later. **(A)** Levels of FABP5 protein were quantified by Western blot. Lanes correspond to individual animals. **(B)** Densitometry analysis of FABP5 levels. Data represents averaged results of individual animals.

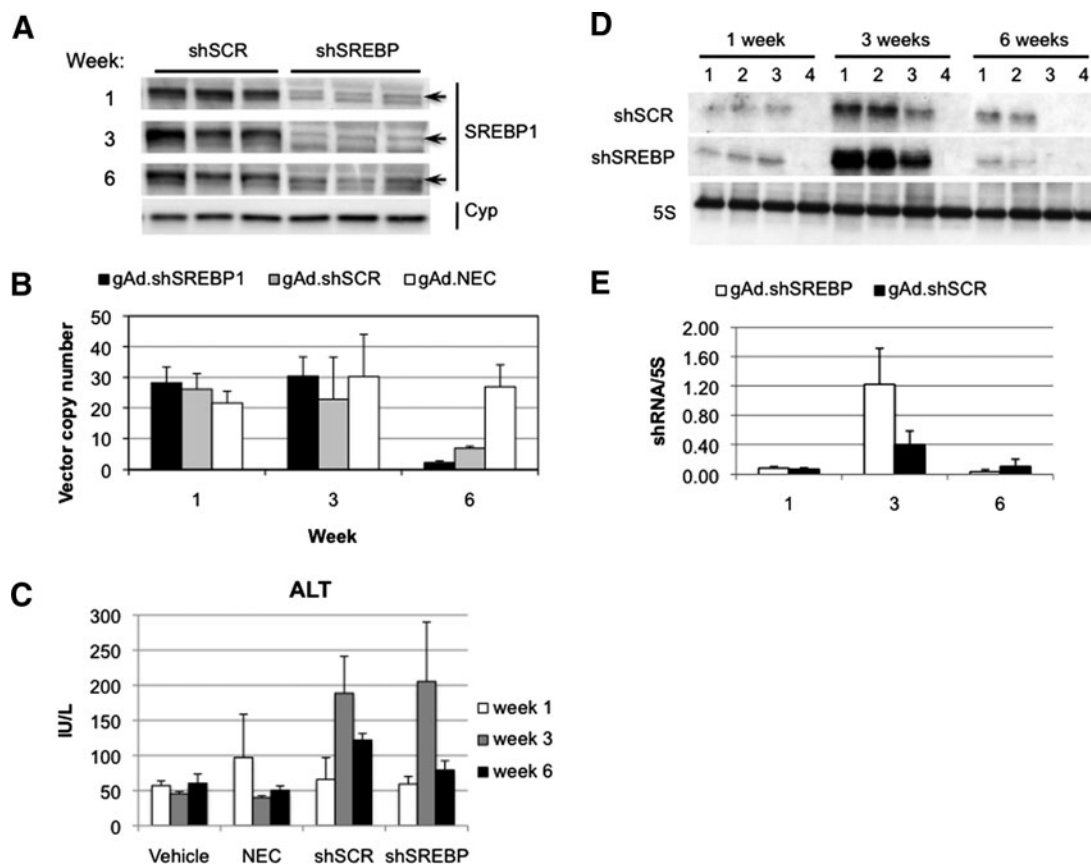


**FIG. 2.** Long-term shRNA expression results in loss of vector genomes. Mice were given  $1 \times 10^{11}$  VP of gAd.shSREBP1, gAd.shSCR, or gAd.NEC, or vehicle, intravenously and were killed 1, 3, and 6 weeks postinjection ( $n = 3$ ). **(A)** SREBP1 gene silencing in the liver was evaluated by Western blot analysis. Lanes correspond to individual animals. Cyp, cyclophilin. **(B)** DNA was isolated from liver and vector genome copy number was analyzed by real-time PCR. DNA vector from the shRNA-expressing vectors decreased between weeks 3 and 6. **(C)** ALT levels were increased over time only in shRNA-expressing groups, not in vehicle and NEC (no expression cassette) groups. **(D)** The microRNA fraction was extracted from liver and shRNA expression was quantified by Northern blot. The level of shRNA expression was highest at 3 weeks and then declined, correlating with the level of vector DNA. Numbers 1 to 3 at the top of the lanes represent mice that received adenoviral vector. Lane 4 represents a mouse treated with vehicle (negative control for shRNA expression). **(E)** Densitometric analysis of shRNA expression relative to 5S.

and levels of shRNA present in the liver were quantified by Northern blot. Interestingly, shRNA levels increased between weeks 1 and 3 and decreased between weeks 3 and 6, correlating with the DNA levels (Fig. 2D and E). Similar results were seen for both shRNA-expressing vectors, regardless of whether the shRNA silenced a gene or not. The accumulation of shRNA between weeks 1 and 3 was surprising, as steady state expression is achieved within a few days after administration of a helper-dependent adenoviral vector expressing a transgene (Morrall *et al.*, 1998).

#### *Loss of transduced hepatocytes is unrelated to saturation of the RNAi machinery*

To study in more detail how this process occurs, mice were given  $1 \times 10^{11}$  VP of gAd.shSREBP1, gAd.shSCR, or gAd.NEC, or vehicle, and killed weekly for 5 consecutive weeks. Mouse body weight did not change in any vector group compared with mice receiving vehicle (Fig. 3A), and none of the animals displayed any signs of sickness or dis-

comfort, indicating that the presence of shRNA-related toxicity in liver did not result in fulminant hepatitis, as had previously been described for adeno-associated virus (AAV)-mediated shRNA expression (Grimm *et al.*, 2006). As previously observed, shRNA accumulation was observed over weeks 1 to 4, and then levels declined gradually (Fig. 3B). This correlated with ALT levels, suggesting liver cell death (Fig. 3C). McBride and colleagues (2008) have shown that expression of shRNA in the brain, using the U6 promoter, leads to toxicity as the result of accumulation of unprocessed hairpin molecules. Contrary to what has been observed in the liver, unprocessed molecules were not detectable in the liver (Fig. 3D). Only mature molecules of the expected 21-nucleotide molecular mass were detected (Fig. 3D), indicating that a mechanism of unprocessed shRNA was unlikely in our study. A second possible cause of toxicity was saturation of the exportin-5 pathway, inducing endogenous microRNA dysregulation and eventually cell death, as previously reported by Grimm and colleagues (2006). Levels of miR-122, a liver-expressed miRNA, were not different in expression among treatments and time points (Fig. 3E),

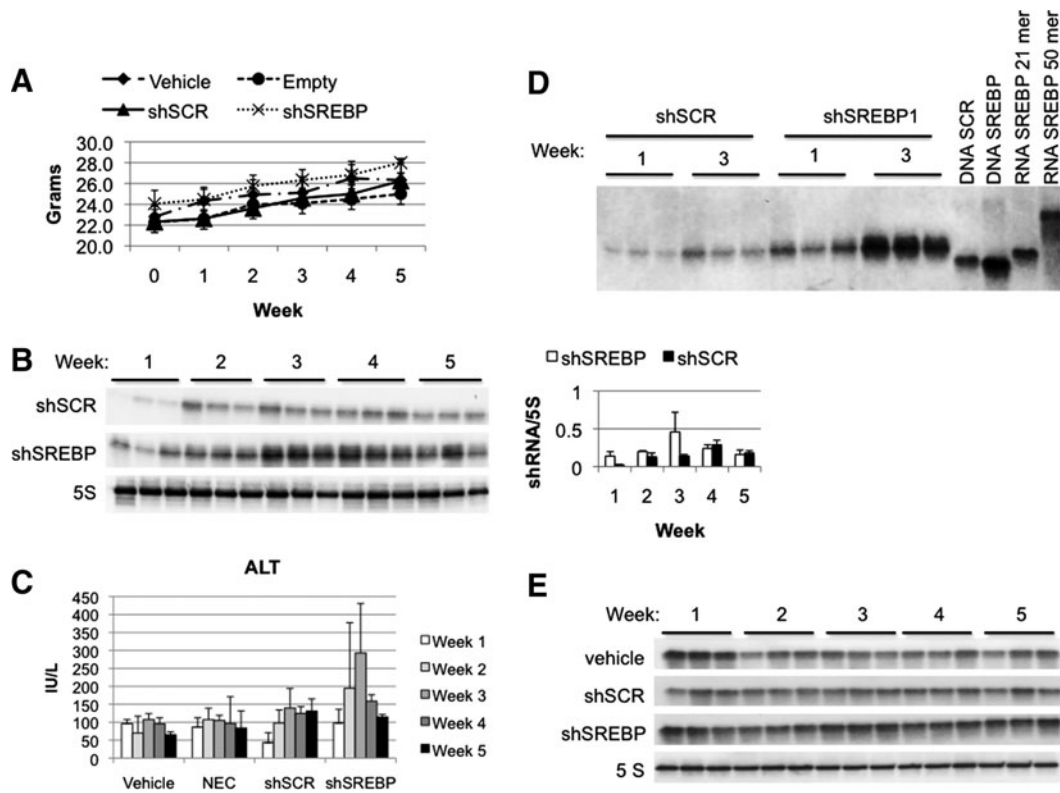


**FIG. 3.** shRNA expression elicits buildup of molecules over time. Mice were administered  $1 \times 10^{11}$  VP of gAd.shSREBP1, gAd.shSCR, or gAd.NEC, or vehicle, and were killed weekly for 5 weeks ( $n = 3$ ). **(A)** Body weight was not altered significantly among treatment groups. **(B)** shRNA expression was quantified by Northern blot (left) and densitometric (right) analysis of shRNA levels. Lanes correspond to individual animals. **(C)** ALT levels. **(D)** Northern blot of the microRNA-enriched fraction, using oligonucleotide (oligo) sequences to detect shSCR or shSREBP molecules. An RNA oligo with the precursor (50-mer) or mature (21-mer) SREBP sequence was spiked into the RNA of a vehicle-treated animal to determine the size of the shRNA molecules present in liver. Only molecules corresponding to the processed shRNA were detected. DNA SCR, scrambled DNA 21-nucleotide antisense sequence; DNA SREBP, SREBP DNA 21-nucleotide antisense sequence; RNA 21-mer, SREBP mature 21-nucleotide RNA oligo; RNA 50-mer, SREBP precursor 50-nucleotide oligo. **(E)** miR-122 levels were not altered at any time points.

suggesting that processing of constitutively expressed shRNA did not saturate exportin-5.

#### Constitutive expression of shRNA induces cell death without interferon response activation

To test whether the accumulation of shRNA on week 3 stimulated the cellular antiviral defense pathway, interferon-stimulated genes (ISGs) *Oas1b* and *Isg56*, were analyzed by real-time RT-PCR. OAS1 (oligoadenylate synthetase-1) induces degradation of RNA through activation of RNase L and subsequent inhibition of protein synthesis (Sledz and Williams, 2004), and *Isg56* functions as a suppressor of viral replication and protein translation (Terenzi *et al.*, 2006). *Oas1b* and *Isg56* levels were not different between the gAd.NEC and vehicle groups (data not shown). No increase was observed between the gAd.shSREBP1 or gAd.shSCR group and the gAd.NEC-treated mice, at any of the time points (Fig. 4). This suggested that the interferon response was not activated in shRNA-expressing mice.

Exonuclease Eri-1 (enhanced RNAi) has been reported to have negative regulatory effects on RNAi (Gabel and Ruvkun, 2008). Eri-1 can degrade the 3' end of siRNA and his-

tone mRNA in *Caenorhabditis elegans*, humans, and fission yeast (Hong *et al.*, 2005; Gabel and Ruvkun, 2008). Administration of high doses of siRNA induces Eri-1 expression in mice (Hong *et al.*, 2005). Thus, we tested whether Eri-1 expression was upregulated in mice expressing shRNA. No increase in Eri-1 mRNA or protein was observed in the gAd.shSREBP or gAd.shSCR group at any time point (Fig. 5).

To determine whether the toxicity correlated with the presence of inflammation, liver sections were stained with hematoxylin-eosin and analyzed by a liver pathologist in a blinded fashion. In agreement with the absence of positive data on the interferon response, no significant inflammation was observed in any of the groups at any time point (Fig. 6). Instead, there was evidence of cellular toxicity, manifested as enlarged hepatocytes that contained pale, ground glass cytoplasmic inclusions. This cellular change was accompanied by numerous apoptotic bodies without accompanying inflammation. Although mitotic figures were present, apoptotic activity outstripped mitotic activity. These histological changes were first observed at a low level at week 3 and involved hepatocytes around the central veins. At weeks 4 and 5, the changes involved increasing numbers of hepatocytes, extending outward toward the portal tracts. The

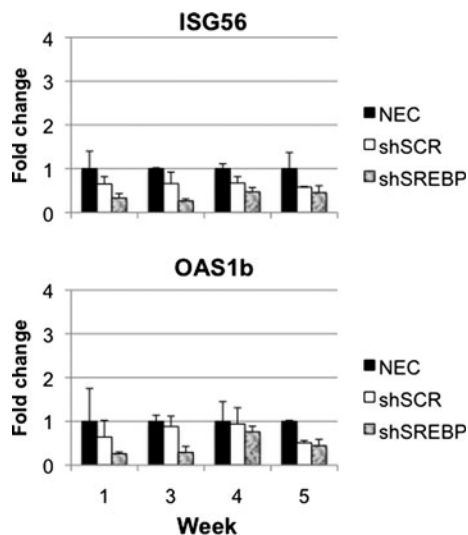


**FIG. 4.** Interferon-stimulated gene (ISG) expression. Mice were treated as described in Fig. 3. Expression levels of two ISG genes, *ISG56* and *Oas1b*, were quantified by real-time RT-PCR. No increase was observed in the gAd.shSREBP and gAd.shSCR groups compared with the gAd.NEC group.

change was both more prominent and more extensive in the gAd.shSREBP1 mice than in the gAd.shSCR animals, extending further out toward the portal tracts in the former group. At week 5, the gAd.shSREBP1 mice showed prominent oval cell proliferation around the portal tracts (Fig. 6). Oval cells are stem cells of the liver that proliferate when the capacity of hepatocytes to divide has been exhausted (Oh *et al.*, 2002). Overall, these observations suggest a process of

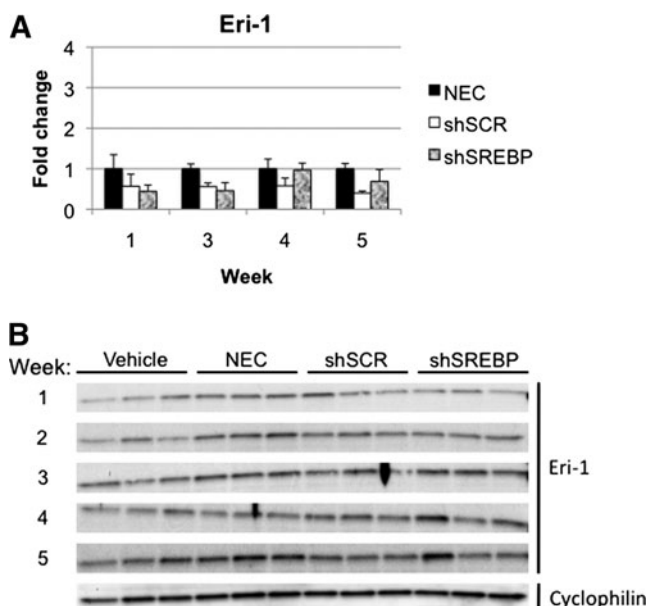


**FIG. 5.** Eri-1 gene and protein analysis. Mice were treated as described in Fig. 3. (A) mRNA expression analysis of Eri-1 in liver by real-time RT-PCR. (B) Western blot quantification of Eri-1 protein. No differences were observed in any group at any time point.

cellular damage triggered by accumulation of mature shRNA molecules. The more extensive damage in mice that received gAd.shSREBP compared with mice that received gAd.shSCR most probably resulted from the higher accumulation of shRNA in the former animals between weeks 1 and 3 (Fig. 3B). This in turn led to oval cell proliferation as the proliferative capacity of damaged hepatocytes was depleted.

#### Microarray analysis suggests role of RNAi components in the pathology

To identify pathways that were altered from over-expressing shRNA, RNA was isolated from livers of mice that received the gAd.NEC, gAd.shSCR, or gAd.shSREBP1 vector and were killed at week 4. This time point was chosen because both groups were expected to have alterations in gene expression induced by shRNA toxicity. We did not observe upregulation of interferon-induced genes (including ISG20, OAS1, and ISG56, which we had previously found highly upregulated when sequences that induce an interferon response are expressed in liver; Witting *et al.*, 2008), confirming that the response is distinct from well-characterized mechanisms of toxicity (Witting *et al.*, 2008). In accordance with the protocol established by Huang and colleagues (2009), functional annotation clustering was performed. This type of analysis organizes redundant/similar/hierarchical terms within a group and allows the investigator to focus on multiple redundant clusters at a glance (Huang *et al.*, 2009). The downregulated genes gave clusters that contained two classes of genes: ribosomal and mitochondrial (Table 2; the full gene list is available on request). Functional annotation clustering for upregulated genes gave clusters in the following categories: cell division (mitogen-activated protein kinase [MAPK] pathway, cytoskeleton organization, cell cycle/growth arrest); endosomal vesicle formation; intracellular protein transport; chromatin-remodeling genes (such as *Baz2a*, a gene shown to inhibit ribosomal RNA [rRNA] synthesis; Zhou *et al.*, 2002); ubiquitination; gene silencing; helicase activity (Table 3; the full gene list is available on request). Genes in more than one of these categories were expected to be dysregulated in the livers of gAd.shSCR- and gAd.shSREBP1-treated mice, given the presence of cell death/division in liver sections (Fig. 6). Interestingly, we observed that several genes in the RNAi pathway were upregulated. Previous studies have shown that siRNA transfection leads to increased expression of TNRC6 (trinucleotide repeat-containing-6), a component of the miRNA pathway (Khan *et al.*, 2009). Our microarray data suggest a possible model in which constitutive expression of shRNA induced expression of molecules of the RNAi pathway such as *Dicer1*, *Mov10*, *Tnrc6b*, and *Cnot1*. Upregulation of these molecules may have initiated a cascade of events through increased recruitment of cellular mRNA-RISC complexes for mRNA degradation, inducing alterations in cellular mRNA levels incompatible with normal function, and causing cell death.

#### Discussion

The speed and cost-effectiveness of *in vivo* gene silencing using viral vectors compared with generating knockout mice has made this system an essential tool to study gene function and in target validation. Several studies have shown the



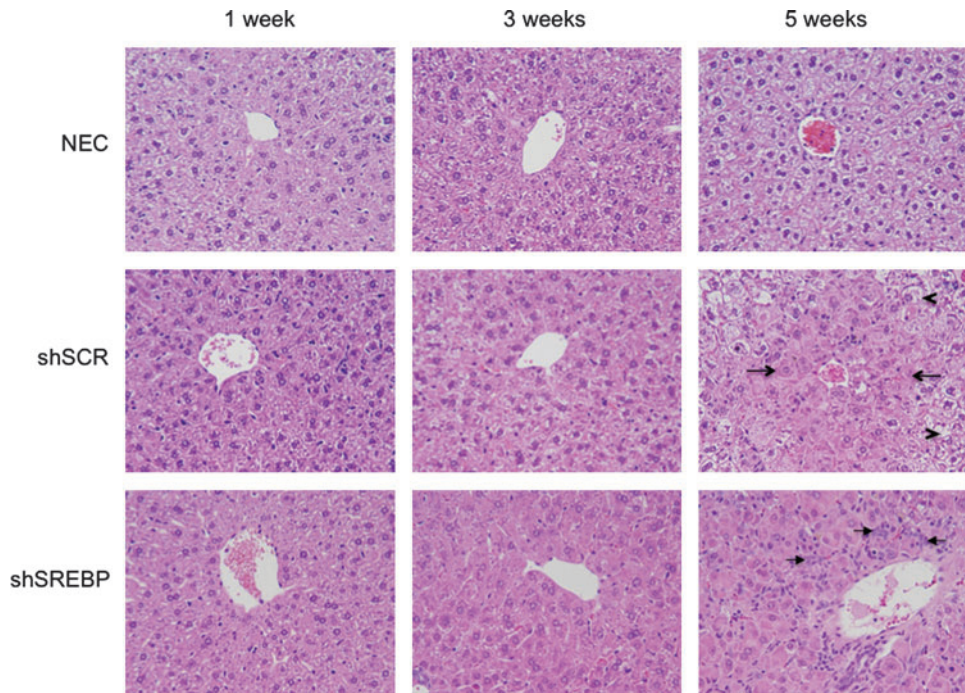


**FIG. 6.** Histology of mouse liver sections. Mice were treated as described in Fig. 3. Liver sections were stained with hematoxylin–eosin and analyzed by a liver pathologist. Panels display the central vein area. In gAd.shSCR-treated liver, dense cells suggestive of having cellular toxicity are denoted by arrows, and normal cells are identified by arrowheads. In animals that received the gAd.shSREBP vector, dense cells were observed almost everywhere in the liver. Arrows indicate the presence of oval cells.

feasibility of this approach to silence liver genes, using AAV and adenoviral vectors (Giering *et al.*, 2008; Hu *et al.*, 2009; Ruiz *et al.*, 2009). We have previously shown that hepatic shRNA expression, using helper-dependent adenoviral vectors, is a feasible approach, and approximately 75–90% gene specific knockdown can be obtained in short-term experiments (1 to 3 weeks) (Witting *et al.*, 2008; Ruiz *et al.*, 2009). In addition, hepatic shRNA expression has the potential to become a treatment for human diseases such as hepatitis B and C virus infection (McCaffrey *et al.*, 2002; Chen *et al.*, 2007). However, the safe application of RNAi as a therapeutic intervention and in functional studies remains an issue, as little is known about the side effects induced by constitutive expression of shRNA *in vivo*.

A previous study investigated the feasibility to use first-generation adenoviral vector-mediated shRNA expression in gene-silencing studies (Narvaiza *et al.*, 2006). This type of vector results in activation of cytotoxic T lymphocyte responses, and clearance of transduced cells occurs soon after vector administration (Yang *et al.*, 1994). Thus, expression of shRNA is expected to be transient and gradually decline as cells are cleared. Expression of shRNA peaked on day 7 and declined afterward, with small amounts of shRNA still being detectable after 150 days (Narvaiza *et al.*, 2006). Target gene silencing was observed for only 12 days (Narvaiza *et al.*, 2006). In contrast, transduction of liver cells by helper-dependent adenoviral vectors results in long-term gene expression (Morral *et al.*, 1999). Thus, shRNA expression with this type of vector is expected to be maintained over time. In the present study we have shown that shRNA expression levels accumulate over a period of 3–4 weeks. Although transient toxicity was induced after this time point, resulting in loss of vector genomes and a subsequent reduction in shRNA levels, gene silencing was maintained for at least 6 weeks. This observation suggests that low amounts of processed shRNA are needed to obtain silencing. It is interesting

that in the study by Narvaiza and colleagues, despite the low level of shRNA detection, no gene silencing was observed beyond 12 days. Given that each shRNA sequence has a different efficacy at silencing the target gene, it is possible that our construct was more efficacious than the one used by Narvaiza and colleagues (2006).

It is remarkable that shRNAs did not reach a steady state level by 7 days after vector administration, as occurs with transgene expression from constitutive promoters, but instead accumulated up to weeks 3 and 4. Three possible scenarios could be devised to explain the increase in shRNA levels after week 1. The first involves downregulation of the U6 promoter (used to express shRNA) on adenovirus entry in liver cells, and subsequent recovery to normal promoter activity after 2–3 weeks. If this scenario were true, the cellular U6 small nuclear RNA (snRNA) gene would also be dysregulated, and levels of this snRNA would gradually increase during weeks 2 and 3 compared with week 1, similar to what was observed with shSREBP1 and shSCR shRNAs. However, we did not observe differences in U6 snRNA levels between time points for any of the groups (data not shown). Thus, accumulation is unlikely to be related to U6 promoter activity. A second possibility is that shRNAs are amplified once the double-stranded RNA is formed in the cell, a mechanism that has been described in *C. elegans* and plants, and more recently in *Drosophila* (Aliyari and Ding, 2009; Lipardi and Paterson, 2009). siRNA amplification occurs as part of the antiviral response and is needed for RNAi in lower eukaryotes. However, dsRNA amplification has never been described in mammals, and the homologous RNA-dependent RNA polymerase (RdRP) required for amplification has not been identified. The third scenario involves multiple rounds of mRNA degradation by the same RISC–shRNA complex. In RNA reactions using HeLa S100 extracts, RISC–let-7 complexes are known to participate in at least 10 rounds of mRNA cleavage (Hutvagner and Zamore,



TABLE 2. GENES DOWNREGULATED MORE THAN 1.5-FOLD

<i>Gene symbol</i>	<i>Gene name</i>	<i>Fold change shSCR and shSREBP1 vs. NEC</i>
<b>Ribosome, structural constituents of ribosome</b>		
Snrpg	Small nuclear ribonucleoprotein polypeptide G	-2.15
Rps25	Ribosomal protein S25	-2.09
Rps12	Ribosomal protein S12	-1.98
Mrpl13	Mitochondrial ribosomal protein L13	-1.95
Rps24	Similar to ribosomal protein S24	-1.89
Rps27	Ribosomal protein S27	-1.87
Rps23	Ribosomal protein S23	-1.83
Mrps33	Mitochondrial ribosomal protein S33; predicted gene 12540	-1.78
Rps7	Ribosomal protein S7	-1.78
Rpl36	Ribosomal protein L36	-1.76
Rpl3	Ribosomal protein L3	-1.74
Rpl11	Ribosomal protein L11	-1.73
Rpl35a	Similar to ribosomal protein L35a	-1.72
Mrps7	Mitochondrial ribosomal protein S7	-1.68
Rpl27a	Ribosomal protein L27a	-1.66
Rps18	Similar to ribosomal protein S18	-1.6
Rpl5	Similar to 60S ribosomal protein L5	-1.58
Rpl14	Ribosomal protein L14	-1.57
Rps9	Ribosomal protein S9; predicted gene 5905	-1.57
<b>Mitochondria</b>		
Ociad2	OCIA domain containing 2	-2.01
Cml1	N-Acetyltransferase 8B; camello-like 1	-1.97
Atp5e	ATP synthase, H <sup>+</sup> transporting, mitochondrial F1 complex, $\epsilon$ subunit	-1.88
1810027O10Rik	RIKEN cDNA 1810027O10 gene	-1.85
Cox4i1	Cytochrome <i>c</i> oxidase subunit IV isoform 1	-1.82
Ndufa4	NADH dehydrogenase (ubiquinone) 1 $\alpha$ subcomplex, 4	-1.81
Ndubf8	NADH dehydrogenase (ubiquinone) 1 $\beta$ subcomplex 8	-1.79
Dnajc19	DnaJ (Hsp40) homolog, subfamily C, member 19	-1.76
Ndubf3	NADH dehydrogenase (ubiquinone) 1 $\beta$ subcomplex 3	-1.75
Cidea	Cell death-inducing DNA fragmentation factor, $\alpha$ subunit-like effector A	-1.63
Cisd1	CDGSH iron sulfur domain 1	-1.61
Atp5l	ATP synthase, H <sup>+</sup> transporting, mitochondrial FO complex, subunit G2, pseudogene	-1.6
Tomm7	Translocase of outer mitochondrial membrane 7 homolog (yeast)	-1.54

2002; Gregory *et al.*, 2005). A single administration of siRNA *in vivo* maintains silencing in tissues for approximately 5–7 days. Thus, it would be expected that constitutive expression of shRNA combined with a multiple-turnover RISC–shRNA complex would lead to increasing levels of shRNA over the course of a few weeks. We believe this is the most plausible explanation to our observations. Future studies will include looking at effects of constitutive expression for multiple months to determine whether silencing can be maintained.

To look into the mechanism causing cellular toxicity, we observed that buildup of mature shRNA molecules occurred between weeks 1 and 4, regardless of whether the shRNA had a target (shSREBP) or not (shSCR) (Fig. 3B). Vector genome copy number was maintained during this time period, and declined afterward. This suggests excess mature hairpin molecules may have elicited a response that resulted in cell death. It is interesting that shRNA sequences without a target are also loaded into RISC and eventually can induce toxic effects similar to those elicited by shRNA molecules with a target mRNA. Higher loss of vector genomes (Fig. 2B) and more severe pathology profiles (including abundant numbers of oval cells around the portal tracts) were observed in the gAd.shSREBP1-treated animals compared with the gAd.shSCR group (Fig. 6). Whether this is related to the fact

that the former has a gene target, and the latter does not, is unknown. A second possibility is that higher levels of shSREBP1 accumulated between weeks 1 and 3 (Figs. 2D and 3B), leading to more cellular damage.

We did not observe accumulation of precursor shRNA molecules or alterations in miR-122 levels (Fig. 3D and E), suggesting that exportin-5 and processing of the precursor shRNA to the cytoplasm were not limiting factors. Interferon-responsive genes were not upregulated (Fig. 4), and inflammatory cells were not present in the liver (Fig. 6), all of which suggest that activation of innate immunity was not the cause of cell death. We have previously observed a strong correlation between induction of an interferon response by shRNA and the presence of inflammation in liver (Witting *et al.*, 2008). Lack of interferon-responsive gene expression was confirmed by microarray analysis of livers of mice killed at week 4. Data generated from this analysis suggest that shRNA expression upregulates genes involved in the RNAi pathway (Table 3). Three of these genes, *Mov10*, *Tnrc6b*, and *Ccr4-Not1*, are located in P-bodies (Table 3). The first two are associated with Argonaute (Ago) in mammalian cells and are required to mediate miRNA-guided mRNA cleavage (Meister *et al.*, 2005). *Mov10* is the human ortholog of *Drosophila* translational repressor Armitage, and has been shown to

TABLE 3. GENES UPREGULATED MORE THAN 1.5 FOLD

<i>Gene symbol</i>	<i>Gene name</i>	<i>Fold change shSCR and shSREBP1 vs. NEC</i>
<b>Posttranscriptional regulation of gene expression</b>		
Mov10	Moloney leukemia virus 10; predicted gene 7357	2.36
Eif4g1	Eukaryotic translation initiation factor 4, $\gamma$ 1	2.14
Mknk2	MAP kinase-interacting serine/threonine kinase 2	2.12
Dicer1	Dicer1, Dcr-1 homolog ( <i>Drosophila</i> )	2.06
App	Amyloid $\beta$ (A4) precursor protein	1.93
Cpeb2	Cytoplasmic polyadenylation element binding protein 2	1.85
Eif4g3	Eukaryotic translation initiation factor 4 $\gamma$ , 3	1.83
Flna	Filamin, alpha	1.79
Zcchc11	Zinc finger, CCHC domain containing 11	1.78
<b>RNA-mediated gene silencing</b>		
Mov10	Moloney leukemia virus 10; predicted gene 7357	2.36
Tnrc6b	Trinucleotide repeat containing 6b	2.07
Dicer1	Dicer1, Dcr-1 homolog ( <i>Drosophila</i> )	2.06
Cnot1	CCR4-NOT transcription complex, subunit 1	1.86
Zcchc11	Zinc finger, CCHC domain containing 11	1.78
<b>Ubiquitin-associated</b>		
Mark2	MAP/microtubule affinity-regulating kinase 2	2.02
Dhx57	DEAH (Asp-Glu-Ala-Asp/His) box polypeptide 57	2.01
Ubqln2	Ubiquilin 2	1.95
Ubap2	Ubiquitin-associated protein 2	1.90
Nbr1	Neighbor of Brca1 gene 1	1.87
<b>Helicase</b>		
Mov10	Moloney leukemia virus 10; predicted gene 7357	2.36
Ddx58	DEAD (Asp-Glu-Ala-Asp) box polypeptide 58	2.12
Dicer1	Dicer1, Dcr-1 homolog ( <i>Drosophila</i> )	2.06
Dhx57	DEAH (Asp-Glu-Ala-Asp/His) box polypeptide 57	2.01
Chd8	Chromodomain helicase DNA binding protein 8	2.00
Smarca4	SWI/SNF related, matrix associated, actin dependent regulator of chromatin, subfamily a, member 4	1.98
Ep400	E1A binding protein p400	1.85
Chd9	Chromodomain helicase DNA binding protein 9	1.77
Ercc2	Excision repair cross-complementing rodent repair deficiency, complementation group 2	1.76
<b>Cell cycle</b>		
Rb1	Retinoblastoma 1	2.67
Ccnb1	Cyclin B1	2.63
Ccnd1	Cyclin D1	2.44
Ep300	E1A binding protein p300	2.12
Ccna2	Cyclin A2	2.08
Plk1	Polo-like kinase 1 ( <i>Drosophila</i> )	2.04
Crebbp	CREB binding protein	1.97
Cdk6	Cyclin-dependent kinase 6	1.82
Smad3	MAD homolog 3 ( <i>Drosophila</i> )	1.68
Smc1a	Structural maintenance of chromosomes 1A	1.64
<b>Endosome/lysosome</b>		
Tpp1	Tripeptidyl peptidase I	2.97
Igf2r	Insulin-like growth factor 2 receptor	2.81
Clcn7	Chloride channel 7	2.41
Siae	Sialic acid acetyltransferase	2.40
Cd68	CD68 antigen	2.18
Slc15a3	Solute carrier family 15, member 3	2.06
Man2b1	Mannosidase 2, $\alpha$ B1	2.01
Ctns	Cystinosis, nephropathic	2.00
Laptm5	Lysosomal-associated protein transmembrane 5	1.99
Arsb	Arylsulfatase B	1.98
Arl8a	ADP-ribosylation factor-like 8A	1.95
Hexb	Hexosaminidase B	1.87
Npc1	Niemann Pick type C1	1.84
Gns	Glucosamine (N-acetyl)-6-sulfatase	1.83
0610031J06Rik	RIKEN cDNA 0610031J06 gene	1.75

(continued)

TABLE 3. (CONTINUED)

<i>Gene symbol</i>	<i>Gene name</i>	<i>Fold change shSCR and shSREBP1 vs. NEC</i>
Lrba	LPS-responsive beige-like anchor	1.75
Ctsa	Cathepsin A	1.74
Gba	Glucosidase, $\beta$ , acid	1.74
Lgmn	Legumain	1.71
Psap	Prosaposin	1.67
Slc29a3	Solute carrier family 29 (nucleoside transporters), member 3	1.58
Vps11	Vacuolar protein sorting 11 (yeast)	1.55
<b>Cytoskeleton</b>		
Spna2	Spectrin $\alpha$ 2	2.33
Utrn	Utrophin	2.28
Vcl	Vinculin	2.26
Mast2	Microtubule associated serine/threonine kinase 2	2.22
Wasf2	WAS protein family, member 2	2.06
Spnb2	Spectrin $\beta$ 2	2
Nf1	Neurofibromatosis 1	1.99
Mapre3	Microtubule-associated protein, RP/EB family, member 3	1.91
Actn4	Actinin $\alpha$ 4	1.84
Phactr4	Phosphatase and actin regulator 4	1.84
Add1	Adducin 1 ( $\alpha$ )	1.83
Tln1	Talin 1	1.83
Actn1	Actinin, $\alpha$ 1	1.81
Flna	Filamin, $\alpha$	1.79
Flnb	Filamin, $\beta$	1.79
Fmn12	Formin-like 2	1.79
Arfgef2	ADP-ribosylation factor guanine nucleotide-exchange factor 2 (brefeldin A-inhibited)	1.78
Ctnna1	Catenin (cadherin associated protein), $\alpha$ 1	1.78
Coro1c	Coronin, actin binding protein 1C; predicted gene 5790	1.77
Eps8l2	EPS8-like 2	1.76
Ablim3	Actin binding LIM protein family, member 3	1.74
Cap1	CAP, adenylate cyclase-associated protein 1 (yeast)	1.72
Diap2	Diaphanous homolog 2 ( <i>Drosophila</i> )	1.72
Myo9b	Myosin IXb	1.71
Msn	Moesin	1.69
Myo9a	Myosin IXa	1.67
Pxk	PX domain containing serine/threonine kinase; similar to PX domain-containing protein kinase-like protein (Modulator of Na,K-ATPase) (MONaKA)	1.65
Myo5b	Myosin VB	1.64
Shroom2	Shroom family member 2	1.63
Macf1	Microtubule-actin crosslinking factor 1	1.62
Pls3	Plastin 3 (T-isoform)	1.59
<b>Chromatin remodeling</b>		
Rb1	Retinoblastoma 1	2.67
Mll5	Myeloid/lymphoid or mixed-lineage leukemia 5	2.12
Ep300	E1A binding protein p300	2.12
Bre	Brain and reproductive organ-expressed protein	2.11
Ncor1	Nuclear receptor co-repressor 1	2.04
Baz2a	Bromodomain adjacent to zinc finger domain, 2A	2.01
Chd8	Chromodomain helicase DNA binding protein 8	2.00
Smarca4	SWI/SNF related, matrix associated, actin dependent regulator of chromatin, subfamily a, member 4	1.98
Crebbp	CREB binding protein	1.97
Huwe1	HECT, UBA, and WWE domain containing 1	1.94
Myst3	MYST histone acetyltransferase (monocytic leukemia) 3	1.87
Ep400	E1A binding protein p400	1.85
Smarcc1	SWI/SNF related, matrix associated, actin dependent regulator of chromatin, subfamily c, member 1	1.84
Eya3	Eyes absent 3 homolog ( <i>Drosophila</i> )	1.82
Setd2	SET domain containing 2	1.80
Bptf	Bromodomain PHD finger transcription factor	1.79
Ezh1	Enhancer of zeste homolog 1 ( <i>Drosophila</i> )	1.78
Chd9	Chromodomain helicase DNA binding protein 9	1.77

(continued)



TABLE 3. (CONTINUED)

<i>Gene symbol</i>	<i>Gene name</i>	<i>Fold change shSCR and shSREBP1 vs. NEC</i>
Nsd1	Nuclear receptor-binding SET-domain protein 1	1.74
Aifm1	Apoptosis-inducing factor, mitochondrion-associated 1	1.73
Ubn1	Ubiquitin 1	1.71
Myst2	MYST histone acetyltransferase 2	1.70
Pbrm1	Polybromo 1	1.69
Smc1a	Structural maintenance of chromosomes 1A	1.64
Rnf40	Ring finger protein 40	1.63
Rcor1	REST corepressor 1	1.57
Rbm14	RNA binding motif protein 14	1.57
<b>Protein transport</b>		
Prpf2	PRA1 domain family 2; predicted gene 4168	2.46
Ap2b1	Adaptor-related protein complex 2, $\beta$ 1 subunit	2.17
Scamp2	Secretory carrier membrane protein 2	2.17
Sec31a	Sec31 homolog A ( <i>S. cerevisiae</i> )	2.11
Mia3	Melanoma inhibitory activity 3	2.07
Pom121	Nuclear pore membrane protein 121	2.06
Slc15a3	Solute carrier family 15, member 3	2.06
Tpr	Similar to nuclear pore complex-associated intranuclear coiled-coil protein TPR; translocated promoter region	2.00
Spm2	Spectrin $\beta$ 2	2.00
Tom1l2	Target of myb1-like 2 (chicken)	1.99
Ap2a1	Adaptor protein complex AP-2, $\alpha$ 1 subunit	1.96
Nup210	Nucleoporin 210	1.94
Ipo13	Importin 13	1.93
Copa	Coatomer protein complex subunit $\alpha$	1.91
Ipo4	Importin 4	1.91
Xpo6	Exportin 6	1.87
Nup214	Nucleoporin 214	1.86
Sec24b	Similar to SEC24 related gene family, member B ( <i>S. cerevisiae</i> )	1.86
Htt	Huntingtin	1.85
Pdcd6ip	Programmed cell death 6 interacting protein	1.85
Actn4	Actinin $\alpha$ 4	1.84
Tln1	Talin 1	1.83
Nsf	N-Ethylmaleimide sensitive fusion protein	1.80
Psen1	Presenilin 1	1.80
Arf3	ADP-ribosylation factor 3	1.80
Hgs	HGF-regulated tyrosine kinase substrate	1.79
Ctnnb1	Catenin (cadherin associated protein), $\beta$ 1	1.79
Flna	Filamin, $\alpha$	1.79
Scamp3	Secretory carrier membrane protein 3	1.78
Ap3b1	Adaptor-related protein complex 3, $\beta$ 1 subunit	1.76
Lrba	LPS-responsive beige-like anchor	1.75
Vps13a	Vacuolar protein sorting 13A (yeast)	1.75
Mon2	MON2 homolog (yeast)	1.73
Os9	Amplified in osteosarcoma	1.72
Ston2	Stonin 2	1.70
Oxa11	Oxidase assembly 1-like	1.69
Rab10	RAB10, member RAS oncogene family	1.67
Ranbp2	RAN binding protein 2	1.67
Ap1b1	Adaptor protein complex AP-1, $\beta$ 1 subunit	1.67
Tnpo2	Transportin 2 (importin 3, karyopherin $\beta$ 2b)	1.66
Scamp4	Secretory carrier membrane protein 4	1.65
Cog1	Component of oligomeric Golgi complex 1	1.64
Myo5b	Myosin VB	1.64
Ap3d1	Adaptor-related protein complex 3, $\delta$ 1 subunit	1.63
Shroom2	Shroom family member 2	1.63
Macf1	Microtubule-actin crosslinking factor 1	1.62
Eif4enif1	Eukaryotic translation initiation factor 4E nuclear import factor 1	1.60
Trpc4ap	Transient receptor potential cation channel, subfamily C, member 4 associated protein	1.59
Vps11	Vacuolar protein sorting 11 (yeast)	1.55
Tom1	Predicted gene 5884; target of myb1 homolog (chicken)	1.51
Tsc2	Tuberous sclerosis 2	1.50

form a complex with RISC, eukaryotic translation initiation factor-6 (eIF6), and ribosomal proteins of the 60S subunit. eIF6 binds to 60S and inhibits assembly of the 60S and 40S ribosome for protein translation (Chendrimada *et al.*, 2007). In neurons, Mov10 degradation has been shown to regulate synaptic plasticity through release of miRNA-mediated translationally repressed mRNA (Banerjee *et al.*, 2009). Tnrc6b is one of three paralogs of GW182 in vertebrates (Ding and Han, 2007) and has been implicated in translational repression (Baillat and Shiekhattar, 2009). Last, Ccr4-Not is a protein present in P-bodies and is involved in mRNA decay through deadenylation (Behm-Ansmant *et al.*, 2006). A model could be envisioned in which upregulation of several genes present in P-bodies may have triggered a cascade of events, starting with inappropriate levels of degradation of miRNA-regulated mRNAs, to a point incompatible with normal hepatocyte function, leading to cell death. Other studies have shown that shRNAs compete with endogenous miRNA for RNAi activity (Castanotto *et al.*, 2007). In addition, saturation of molecules in the RNAi pathway has previously been shown to lead to toxicity (Grimm *et al.*, 2006, 2010). Saturation of exportin-5 results in fulminant hepatitis (Grimm *et al.*, 2006), and saturation of Ago proteins, in particular Ago-2, induces toxicity and cell death (Grimm *et al.*, 2010). Increasing Ago-2 activity alleviates the toxicity and extends RNAi (Diederichs *et al.*, 2008; Grimm *et al.*, 2010). Nevertheless, Grimm and colleagues showed that the most efficient way to reduce cytotoxicity and prolong gene silencing was to use weaker promoters that resulted in lower levels of shRNA (Grimm *et al.*, 2010). Kahn and colleagues have reported that transfection of small RNAs into cells results in increased expression of miRNA-regulated genes, likely through saturation of RNAi components downstream from exportin-5, such as Argonaute proteins and TRBP (HIV-1 *trans*-activating response [TAR] RNA-binding protein) (Khan *et al.*, 2009). One of the upregulated genes was TNRC6 (Khan *et al.*, 2009), one of the three GW182 paralogs. The data generated in our study suggests a model in which several genes in the RNAi pathway were upregulated, three of which are associated with P-bodies. Additional studies need to be conducted to confirm this model and whether increased P-body function is sufficient to induce toxicity. Last, it is also conceivable that downregulation of cellular gene expression due to off-target effects contributed to induce toxic effects and cell death. On the basis of all these studies, constitutive shRNA expression may result in toxicity from a combination of mechanisms, including saturation of the exportin-5 pathway, competition of shRNA with endogenous miRNA for RISC or for other molecules downstream from exportin-5, upregulation of genes in the RNAi pathway, or off-target effects, all of which can lead to dysregulated expression of cellular genes and potentially induce cell death.

In conclusion, expression of shRNA from helper-dependent adenoviral vectors leads to a high level of silencing for multiple weeks *in vivo*. Despite silencing, expression of shRNA results in cellular apoptosis and loss of vector genomes, likely because of excess accumulation of mature shRNA molecules. Our data have implications for the safe design of shRNA expression cassettes, and argue for close monitoring for signs of toxicity at multiple time points. This is particularly important for studies in which cell death/survival is an outcome of the gene-silencing treatment. As also observed by other groups

(Grimm *et al.*, 2010), our data suggest that the development of future vectors should include expression cassettes with lower promoter strength or inducible systems, to provide safer tools for gene function studies, gene target validation, and for clinical applications.

### Acknowledgments

This research was supported by grants from the National Institutes of Health (DK069432-01, DK078595); American Diabetes Association (1-08-RA-135); and INGEN (Indiana Genomics Initiative of Indiana University supported in part by Lilly Endowment Inc.). The authors thank Dr. Jeanette McClintick for assistance on microarray analysis, which was carried out using the facilities of the Center for Medical Genomics at Indiana University School of Medicine, supported in part by a grant from the Indiana 21st Century Research and Technology Fund, and by INGEN. Miwon Ahn was supported by the T32-Indiana University Diabetes and Obesity Research Training Program (DK064466), and Scott R. Witting by a postdoctoral fellowship from the American Heart Association.

### Author Disclosure Statement

No competing financial interests exist.

### References

- Aliyari, R., and Ding, S.W. (2009). RNA-based viral immunity initiated by the Dicer family of host immune receptors. *Immunol. Rev.* 227, 176–188.
- Baillat, D., and Shiekhattar, R. (2009). Functional dissection of the human TNRC6 (GW182-related) family of proteins. *Mol. Cell Biol.* 29, 4144–4155.
- Banerjee, S., Neveu, P., Kosik, K.S. (2009). A coordinated local translational control point at the synapse involving relief from silencing and MOV10 degradation. *Neuron* 64, 871–884.
- Behm-Ansmant, I., Rehwinkel, J., Doerks, T., *et al.* (2006). mRNA degradation by miRNAs and GW182 requires both CCR4:NOT deadenylase and DCP1:DCP2 decapping complexes. *Genes Dev.* 20, 1885–1898.
- Boudreau, R.L., McBride, J.L., Martins, I., *et al.* (2009). Nonallele-specific silencing of mutant and wild-type huntingtin demonstrates therapeutic efficacy in Huntington's disease mice. *Mol. Ther.* 17, 1053–1063.
- Brummelkamp, T.R., Bernards, R., and Agami, R. (2002). A system for stable expression of short interfering RNAs in mammalian cells. *Science* 296, 550–553.
- Castanotto, D., Sakurai, K., Lingeman, R., *et al.* (2007). Combinatorial delivery of small interfering RNAs reduces RNAi efficacy by selective incorporation into RISC. *Nucleic Acids Res.* 35, 5154–5164.
- Chen, C.C., Ko, T.M., Ma, H.I., *et al.* (2007). Long-term inhibition of hepatitis B virus in transgenic mice by double-stranded adeno-associated virus 8-delivered short hairpin RNA. *Gene Ther.* 14, 11–19.
- Chendrimada, T.P., Finn, K.J., Ji, X., *et al.* (2007). MicroRNA silencing through RISC recruitment of eIF6. *Nature* 447, 823–828.
- Colombo, R., and Moll, J. (2008). Target validation to biomarker development: Focus on RNA interference. *Mol. Diagn. Ther.* 12, 63–70.
- Diederichs, S., Jung, S., Rothenberg, S.M., *et al.* (2008). Coexpression of Argonaute-2 enhances RNA interference toward

- perfect match binding sites. *Proc. Natl. Acad. Sci. U.S.A.* 105, 9284–9289.
- Ding, L., and Han, M. (2007). GW182 family proteins are crucial for microRNA-mediated gene silencing. *Trends Cell Biol.* 17, 411–416.
- Gabel, H.W., and Ruvkun, G. (2008). The exonuclease ERI-1 has a conserved dual role in 5.8S rRNA processing and RNAi. *Nat. Struct. Mol. Biol.* 15, 531–533.
- Giering, J.C., Grimm, D., Storm, T.A., and Kay, M.A. (2008). Expression of shRNA from a tissue-specific Pol II promoter is an effective and safe RNAi therapeutic. *Mol. Ther.* 16, 1630–1636.
- Gregory, R.I., Chendrimada, T.P., Cooch, N., and Shiekhattar, R. (2005). Human RISC couples microRNA biogenesis and posttranscriptional gene silencing. *Cell* 123, 631–640.
- Grimm, D., and Kay, M.A. (2006). Therapeutic short hairpin RNA expression in the liver: Viral targets and vectors. *Gene Ther.* 13, 563–575.
- Grimm, D., Streetz, K.L., Jopling, C.L., *et al.* (2006). Fatality in mice due to oversaturation of cellular microRNA/short hairpin RNA pathways. *Nature* 441, 537–541.
- Grimm, D., Wang, L., Lee, J.S., *et al.* (2010). Argonaute proteins are key determinants of RNAi efficacy, toxicity, and persistence in the adult mouse liver. *J. Clin. Invest.* 120, 3106–3119.
- Hegenbarth, S., Gerolami, R., Protzer, U., *et al.* (2000). Liver sinusoidal endothelial cells are not permissive for adenovirus type 5. *Hum. Gene Ther.* 11, 481–486.
- Hong, J., Qian, Z., Shen, S., *et al.* (2005). High doses of siRNAs induce *eri-1* and *adar-1* gene expression and reduce the efficiency of RNA interference in the mouse. *Biochem. J.* 390, 675–679.
- Hu, P.F., Chen, H., Zhong, W., *et al.* (2009). Adenovirus-mediated transfer of siRNA against PAI-1 mRNA ameliorates hepatic fibrosis in rats. *J. Hepatol.* 51, 102–113.
- Huang, D.W., Sherman, B.T., and Lempicki, R.A. (2009). Systematic and integrative analysis of large gene lists using DAVID bioinformatics resources. *Nat. Protoc.* 4, 44–57.
- Hutvagner, G., and Zamore, P.D. (2002). A microRNA in a multiple-turnover RNAi enzyme complex. *Science* 297, 2056–2060.
- Inagaki, Y., Kushida, M., Higashi, K., *et al.* (2005). Cell type-specific intervention of transforming growth factor  $\beta$ /Smad signaling suppresses collagen gene expression and hepatic fibrosis in mice. *Gastroenterology* 129, 259–268.
- Khan, A.A., Betel, D., Miller, M.L., *et al.* (2009). Transfection of small RNAs globally perturbs gene regulation by endogenous microRNAs. *Nat. Biotechnol.* 27, 549–555.
- Lipardi, C., and Paterson, B.M. (2009). Identification of an RNA-dependent RNA polymerase in *Drosophila* involved in RNAi and transposon suppression. *Proc. Natl. Acad. Sci. U.S.A.* 106, 15645–15650.
- Liu, J., Carmell, M.A., Rivas, F.V., *et al.* (2004). Argonaute2 is the catalytic engine of mammalian RNAi. *Science* 305, 1437–1441.
- Lu, S., and Cullen, B.R. (2004). Adenovirus VA1 noncoding RNA can inhibit small interfering RNA and microRNA biogenesis. *J. Virol.* 78, 12868–12876.
- Matranga, C., Tomari, Y., Shin, C., *et al.* (2005). Passenger-strand cleavage facilitates assembly of siRNA into Ago2-containing RNAi enzyme complexes. *Cell* 123, 607–620.
- McBride, J.L., Boudreau, R.L., Harper, S.Q., *et al.* (2008). Artificial miRNAs mitigate shRNA-mediated toxicity in the brain: Implications for the therapeutic development of RNAi. *Proc. Natl. Acad. Sci. U.S.A.* 105, 5868–5873.
- McCaffrey, A.P., Meuse, L., Pham, T.T., *et al.* (2002). RNA interference in adult mice. *Nature* 418, 38–39.
- McIntyre, G.J., and Fanning, G.C. (2006). Design and cloning strategies for constructing shRNA expression vectors. *BMC Biotechnol.* 6, 1.
- Meister, G., Landthaler, M., Peters, L., *et al.* (2005). Identification of novel Argonaute-associated proteins. *Curr. Biol.* 15, 2149–2155.
- Morral, N., O'Neal, W., Zhou, H., *et al.* (1997). Immune responses to reporter proteins and high viral dose limit duration of expression with adenoviral vectors: Comparison of E2a wild type and E2a deleted vectors. *Hum. Gene Ther.* 8, 1275–1286.
- Morral, N., Parks, R., Zhou, H., *et al.* (1998). High doses of a helper-dependent adenoviral vector yield supraphysiological levels of  $\alpha_1$ -antitrypsin with negligible toxicity. *Hum. Gene Ther.* 9, 2709–2716.
- Morral, N., O'Neal, W., Rice, K., *et al.* (1999). Administration of helper-dependent adenoviral vectors and sequential delivery of different vector serotype for long-term liver-directed gene transfer in baboons. *Proc. Natl. Acad. Sci. U.S.A.* 96, 12816–12821.
- Narvaiza, I., Aparicio, O., Vera, M., *et al.* (2006). Effect of adenovirus-mediated RNA interference on endogenous microRNAs in a mouse model of multidrug resistance protein 2 gene silencing. *J. Virol.* 80, 12236–12247.
- O'Neal, W.K., Zhou, H., Morral, N., *et al.* (2000). Toxicity associated with repeated administration of first-generation adenovirus vectors does not occur with a helper-dependent vector. *Mol. Med.* 6, 179–195.
- Oh, S.H., Hatch, H.M., and Petersen, B.E. (2002). Hepatic oval “stem” cell in liver regeneration. *Semin. Cell Dev. Biol.* 13, 405–409.
- Parks, R.J., Chen, L., Anton, M., *et al.* (1996). A helper-dependent adenovirus vector system: Removal of helper virus by Cre-mediated excision of the viral packaging signal. *Proc. Natl. Acad. Sci. U.S.A.* 93, 13565–13570.
- Persengiev, S.P., Zhu, X., and Green, M.R. (2004). Nonspecific, concentration-dependent stimulation and repression of mammalian gene expression by small interfering RNAs (siRNAs). *RNA* 10, 12–18.
- Reynolds, A., Anderson, E.M., Vermeulen, A., *et al.* (2006). Induction of the interferon response by siRNA is cell type- and duplex length-dependent. *RNA* 12, 988–993.
- Robbins, M., Judge, A., Ambegia, E., *et al.* (2008). Misinterpreting the therapeutic effects of small interfering RNA caused by immune stimulation. *Hum. Gene Ther.* 19, 991–999.
- Ruiz, R., Witting, S.R., Saxena, R., and Morral, N. (2009). Robust hepatic gene silencing for functional studies using helper-dependent adenovirus vectors. *Hum. Gene Ther.* 20, 87–94.
- Schiedner, G., Morral, N., Parks, R., *et al.* (1998). Genomic DNA transfer with a high-capacity adenovirus vector results in improved *in vivo* gene expression and decreased toxicity. *Nat. Genet.* 18, 180–183.
- Sledz, C.A., and Williams, B.R. (2004). RNA interference and double-stranded-RNA-activated pathways. *Biochem. Soc. Trans.* 32, 952–956.
- Song, J.J., Smith, S.K., Hannon, G.J., and Joshua-Tor, L. (2004). Crystal structure of Argonaute and its implications for RISC slicer activity. *Science* 305, 1434–1437.
- Stratford-Perricaudet, L.D., Levrero, M., Chase, J.F., *et al.* (1990). Evaluation of the transfer and expression in mice of an enzyme-encoding gene using a human adenovirus vector. *Hum. Gene Ther.* 1, 241–256.



- Taniguchi, C.M., Ueki, K., and Kahn, R. (2005). Complementary roles of IRS-1 and IRS-2 in the hepatic regulation of metabolism. *J. Clin. Invest.* 115, 718–727.
- Terenzi, F., Hui, D.J., Merrick, W.C., and Sen, G.C. (2006). Distinct induction patterns and functions of two closely related interferon-inducible human genes, *ISG54* and *ISG56*. *J. Biol. Chem.* 281, 34064–34071.
- Wheeler, M.D., Yamashina, S., Froh, M., *et al.* (2001). Adenoviral gene delivery can inactivate Kupffer cells: Role of oxidants in NF- $\kappa$ B activation and cytokine production. *J. Leukoc. Biol.* 69, 622–630.
- Witting, S.R., Brown, M., Saxena, R., *et al.* (2008). Helper-dependent adenovirus-mediated short hairpin RNA expression in the liver activates the interferon response. *J. Biol. Chem.* 283, 2120–2128.
- Xia, H., Mao, Q., Paulson, H.L., and Davidson, B.L. (2002). siRNA-mediated gene silencing *in vitro* and *in vivo*. *Nat. Biotechnol.* 20, 1006–1010.
- Yang, Y., Li, Q., Ertl, H.C., and Wilson, J.M. (1994). Cellular immunity to viral antigens limits E1-deleted adenoviruses for gene therapy. *Proc. Natl. Acad. Sci. U.S.A.* 91, 4407–4411.
- Zhou, Y., Santoro, R., and Grummt, I. (2002). The chromatin remodeling complex NoRC targets HDAC1 to the ribosomal gene promoter and represses RNA polymerase I transcription. *EMBO J.* 21, 4632–4640.

Address correspondence to:

Dr. Núria Morral

Department of Medical and Molecular Genetics

Indiana University School of Medicine

975 West Walnut Street, Room IB 130

Indianapolis, IN 46202

E-mail: nmorrals@iupui.edu

Received for publication December 10, 2010;

accepted after revision July 22, 2011.

Published online: July 22, 2011.

